Mapping and Localization using Multispectral Imaging of the Soil

Stefan Glaser, Alexander Schaefer, Wolfram Burgard

***Abstract*— Multispectral analysis of the soil can provide rich information about its physical and chemical properties. In this study, we show how to leverage this information for localization purposes. We describe a map representation suitable for soil properties derived from multispectral images and demonstrate how to integrate such maps in a localization approach. Experimental results demonstrate the performance of the proposed method, reaching a localization accuracy comparable to a GPS-based solution. Apart from agricultural robots, the proposed method may also be suitable for mining and extra-terrestrial applications.**

I. INTRODUCTION

Localizing agricultural robots is one of the fundamental challenges in precision agriculture. Popular solutions are based on GNSS (Global Navigation Satellite System), INS (inertial navigation system) and wheel odometry [1]. While GNSS is a very powerful tool, it is affected by signal blocking and multipathing, arising in urban, heavily forested, or mountainous environments. As a result, the accuracy and robustness of GNSS typically vary depending on the actual location and environment.

Due to these limitations, Cornick et. al. [2] recently proposed a novel localization approach for ground vehicles, in which they use a ground-penetrating radar system to measure and map various subterranean features of the ground underneath the vehicle. Levison and Thrun [3] successfully build probabilistic ground surface intensity maps captured by lidar sensors to achieve a high precision localization.

In precision agriculture, multispectral and hyperspectral cameras are widely used to map and monitor vegetation and soil conditions. So-called vegetation indices [4] were developed to determine the amount and measure the condition of the vegetation within an image. In addition to that, multispectral analysis of soil samples allows the characterization of soil compositions and properties [5], [6]. However, such maps are typically used to coordinate individual plant treatments like fertilizer distribution, rather than localizing a vehicle on the field.

In this study, we explore the possibility of using soil properties derived from multispectral images of the top soil surface in the context of mapping and localization. The investigated soil properties in this study are represented by the Normalized Difference Vegetation Index (NDVI) [7]. All experiments were conducted on the sugar beets dataset [8].

All authors are with the Department of Computer Science, University of Freiburg {glasers, aschaef, burgard} @cs.uni-freiburg.de

This work has partly been supported by the European Union under grant number H2020-ICT-644227-FLOURISH.

II. APPROACH

The robot in the sugar beets dataset operates along individual rows or lanes within the field, which allows the localization and mapping problem to be broken down to one dimension. As the robot moves along a row of the field, it simultaneously captures RGB and near-infrared (NIR) images of the ground underneath it. A pre-processing step calculates the mean NDVI value over each image pair, while excluding vegetation pixels with a NDVI value greater than 0.2. The resulting mean NDVI values are then used for mapping and for localizing the robot relative to a previously acquired probabilistic NDVI map.

A. MAPPING

In our scenario, spectral indices are real-valued random variables, measured at different locations. We use a special form of Gaussian process regression called Kriging [9] to approximate the true NDVI functions along the rows of the field. Assuming a locally linear trend in the observed data, Kriging provides the best linear prediction of the intermediate values along with a prediction variance. Given a set of mean NDVI measurements Z and measurement locations X (obtained via Real Time Kinematic (RTK) GPS), the Kriging model estimates the expected NDVI function $\mu(X, Z, x)$ along with the prediction standard deviation $\sigma(X, Z, x)$ for arbitrary locations x. Figure 1 shows an example NDVI map.

The investigation of the mean NDVI values along the same row at different days revealed that even though they follow a similar shape, they have different absolute offsets. As a

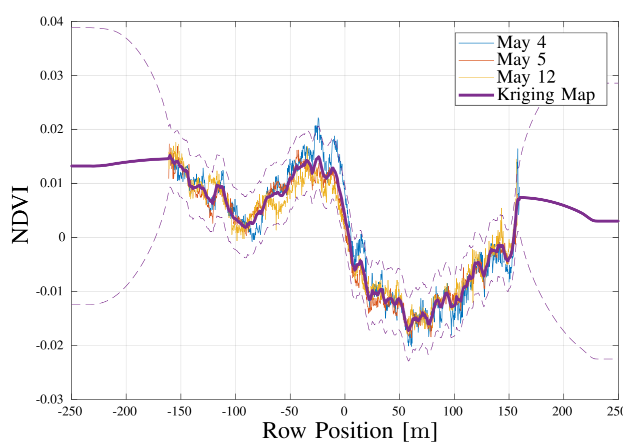

Fig. 1: 1-D mean NDVI map obtained via Kriging (purple line with confidence interval indicated by the dashed lines) along with the three raw measurement series (from May 4, 5 and 12, 2016) used for map construction.

result, all measurement series are shifted by their negative mean value prior to the mapping procedure.

B. LOCALIZATION

Localizing the robot relative to the spectral index map is achieved by employing a particle filter based on wheel odometry, RGB-NIR images and the probabilistic index map. As the mean NDVI value offset is unknown during localization, each particle represents a combination of a possible position and mean NDVI value offset. The motion model uses the current velocity reported by the wheel odometry with added Gaussian noise ($\mu_v = 0$ and $\sigma_v = 0.36\,\mathrm{m}$) to predict the future positions of the particles. The measurement model calculates the likelihood of the currently measured mean NDVI value given the map and particle positions:

$$p(z|X, Z, x) = \mathcal{N}(z; \mu(X, Z, x), \sigma^2(X, Z, x))$$

where X and Z represent the training data as described above, x is the particle position, and z is the current mean NDVI measurement.

III. EXPERIMENTAL RESULTS

To evaluate the performance of the proposed method, we conducted two experiments using the sugar beets dataset [8].

For this dataset, wheel odometry of the robot was recorded at $20\,\mathrm{Hz}$, the JAI AD-130GE multispectral camera feed at $1\,\mathrm{Hz}$ and ground truth location information from the Leica RTK GPS at $10\,\mathrm{Hz}$. The JAI camera images cover a region of $24\,\mathrm{cm} \times 31\,\mathrm{cm}$ at a resolution of approximatively $3\,\mathrm{px/mm}$. Apart from that, the dataset also provides a Ublox EVK7-P GPS module recorded at $4\,\mathrm{Hz}$.

In the first experiment, the position tracking performance of the proposed localization approach is compared against pure odometry and a particle filter based on odometry and the Ublox GPS module (see Table I). The image frequency in this scenario is $0.5\,\mathrm{Hz}$, as the available RGB-NIR images are split into training images used for map construction and evaluation images used during localization. Each approach is reinitialized with the true position at the beginning of each measurement series of a row of the field. In comparison to pure odometry, the proposed method is able to reduce the mean absolute position error from $4.32\,\mathrm{m}$ to $0.93\,\mathrm{m}$, which is only $7\,\mathrm{cm}$ less accurate than the GPS-based solution.

	Odometry	Odometry + GPS	Odometry + NDVI map
Mean abs. position error [m]	4.32	0.86	0.93
Position error std. dev. [m]	5.08	0.78	1.37

TABLE I: 1-D position tracking performance of pure odometry vs. odometry and GPS-based particle filter vs. odometry and mean NDVI map based particle filter. Results are obtained from 79 measurement series, recorded over a period of 29 days, while traveling a total distance of almost $25\,\mathrm{km}$.

In the second experiment, the particle filter has to recover the initially unknown position and direction of the robot as well as the mean NDVI value offset at the same time. The

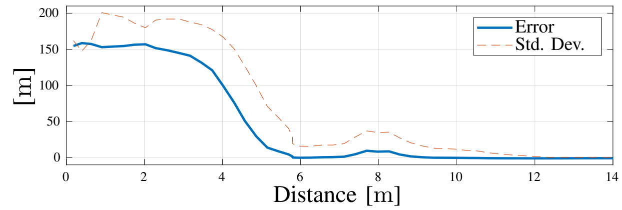

Fig. 2: Mean particle position error (solid line) and particle position standard deviation (dashed line) over traveled distance, for the NDVI map based particle filter solving the global localization problem. The particle filter requires the robot to travel a certain distance before it is able to correlate measurements with the map. After that, it quickly converges to the true position, while maintaining multiple possible solutions due to map symmetries.

map for this experiment is created from two measurement series recorded on May 4 and 5, 2016, while the localization is performed on a third measurement series recorded on May 12. The evolution of the particle filter is illustrated in Figure 2. After incorporating 45 mean NDVI measurements over a distance of $12.5\,\mathrm{m}$, $95\,\%$ of the particles are within $2\,\mathrm{m}$ around the true position of the robot, pointing into the correct direction. At this point in time, the predicted position is $7.5\,\mathrm{cm}$ off the true position, with a standard deviation of $47\,\mathrm{cm}$. The mean absolute position error along the remaining $306\,\mathrm{m}$ of the measurement series is $1.36\,\mathrm{m}$ with a position error standard deviation of $1.62\,\mathrm{m}$.

IV. FUTURE WORK

As the concept behind the proposed approach is not limited to one dimension, we intend to apply it to two dimensions. Apart from that, we will investigate other indices than the NDVI, as there exists a rich variety of spectral indices, potentially encoding different aspects of the soil.

REFERENCES

[1] S. Kennedy and J. Rossi, "Performance of a deeply coupled commercial grade GPS/INS system from KVH and NovAtel Inc.," 06 2008.

[2] C. Matthew, K. Jeffrey, S. Byron, and Z. Beijia, "Localizing Ground Penetrating RADAR: A Step Toward Robust Autonomous Ground Vehicle Localization," *Journal of Field Robotics*, vol. 33, no. 1, 2015.

[3] J. Levinson and S. Thrun, "Robust Vehicle Localization in Urban Environments Using Probabilistic Maps," 06 2010.

[4] B. Abdou, D. Morin, F. Bonn, and A. Huete, "A Review of Vegetation Indices," *Remote Sensing Reviews*, vol. 13, pp. 95–120, 01 1996.

[5] R. V. Rossel, D. Walvoort, A. McBratney, L. Janik, and J. Skjemstad, "Visible, near infrared, mid infrared or combined diffuse reflectance spectroscopy for simultaneous assessment of various soil properties," *Geoderma*, vol. 131, no. 1, pp. 59 – 75, 2006.

[6] W. D. Hively, G. W. McCarty, J. B. Reeves, M. W. Lang, R. A. Oesterling, and S. R. Delwiche, "Use of Airborne Hyperspectral Imagery to Map Soil Properties in Tilled Agricultural Fields," *Applied and Environmental Soil Science*, vol. 2011, 2011.

[7] J. W. Rouse, "Monitoring the vernal advancement and retrogradation (green wave effect) of natural vegetation," *NASA/GSFCT Report*, 1974.

[8] N. Chebrolu, P. Lottes, A. Schaefer, W. Winterhalter, W. Burgard, and C. Stachniss, "Agricultural Robot Dataset for Plant Classification, Localization and Mapping on Sugar Beet Fields," *The International Journal of Robotics Research*, 2017.

[9] T. Hengl, *A Practical Guide to Geostatistical Mapping of Environmental Variables*. Office for Official Publications of the European Communities, 2007.